

Calculation of radiative heat flux on irregular boundaries in participating media

Yu-Jia Sun(孙玉佳)[1] and Shu Zheng(郑树)[2,†]

Citation: Chin. Phys. B, 2020, 29 (**12**): 124401. DOI: 10.1088/1674-1056/abb22a
Journal homepage: http://cpb.iphy.ac.cn; http://iopscience.iop.org/cpb

What follows is a list of articles you may be interested in

Infrared cooling properties of cordierite

Si-Heng Chen(陈思衡), Xiao-Xiong Wang(王晓雄), Guang-Di Nie(乜广弟), Qi Liu(刘奇), Jin-Xia Sui(隋金霞), Chao Song(宋超), Jian-Wei Zhu(朱建伟), Jie Fu(付洁), Jun-Cheng Zhang(张君诚), Xu Yan(闫旭), Yun-Ze Long(龙云泽)
Chin. Phys. B, 2019, 28 (**6**): 064401. DOI: 10.1088/1674-1056/28/6/064401

Contribution of terahertz waves to near-field radiative heat transfer between graphene-based hyperbolic metamaterials

Qi-Mei Zhao(赵启梅), Tong-Biao Wang(王同标), De-Jian Zhang(张德建), Wen-Xing Liu(刘文兴), Tian-Bao Yu(于天宝), Qing-Hua Liao(廖清华), Nian-Hua Liu(刘念华)
Chin. Phys. B, 2018, 27 (**9**): 094401. DOI: 10.1088/1674-1056/27/9/094401

Reconstruction model for temperature and concentration profiles of soot and metal-oxide nanoparticles in a nanofluid fuel flame by using a CCD camera

Guannan Liu(刘冠楠), Dong Liu(刘冬)
Chin. Phys. B, 2018, 27 (**5**): 054401. DOI: 10.1088/1674-1056/27/5/054401

Simultaneous reconstruction of temperature distribution and radiative properties in participating media using a hybrid LSQR–PSO algorithm

Niu Chun-Yang, Qi Hong, Huang Xing, Ruan Li-Ming, Wang Wei, Tan He-Ping
Chin. Phys. B, 2015, 24 (**11**): 114401. DOI: 10.1088/1674-1056/24/11/114401

Spectral enhancement of thermal radiation by laser fabricating grating structure on nickel surface

Liu Song, Liu Shi-Bing
Chin. Phys. B, 2015, 24 (**5**): 054401. DOI: 10.1088/1674-1056/24/5/054401

Calculation of radiative heat flux on irregular boundaries in participating media*

Yu-Jia Sun(孙玉佳)[1] and Shu Zheng(郑树)[2,†]

[1] School of Atmospheric Physics, Nanjing University of Information Science and Technology, Nanjing 210044, China
[2] National Engineering Laboratory for Biomass Power Generation Equipment, North China Electric Power University, Beijing 102206, China

(Received 17 May 2020; revised manuscript received 1 July 2020; accepted manuscript online 25 August 2020)

Radiative heat flux at wall boundaries is important for its thermal design. Numerical methods based on structured grids are becoming trendy due to their simplicity and efficiency. Existing radiative transfer equation solvers produce oscillating radiative heat flux at the irregular boundary if they are based on structured grids. Reverse Monte Carlo method and analytical discrete ordinates method are adopted to calculate the radiative heat flux at complex boundaries. The results show that the reverse Monte Carlo method can generate a smooth radiative heat flux profile and it is smoother with larger energy bundles. The results from the analytical discrete ordinates method show that the fluctuations are due to the ray effect. For the total or the mean radiative heat flux, the results from the analytical discrete ordinates method are very close to those from the reverse Monte Carlo method.

Keywords: radiative heat flux, reverse Monte Carlo, irregular boundary

PACS: 44.40.+a **DOI:** 10.1088/1674-1056/abb22a

1. Introduction

Radiation heat transfer plays a dominant role in high-temperature systems, such as furnace,[1–3] fluidized bed,[4,5] flames,[6–10] combustion diagnostics.[11–13] Radiative energy exchange between the participating medium and the wall surface is the most important information for thermal design of these systems. Hence, it is of high significance to accurately predict the radiative heat flux along the wall surface.

For general problems, unstructured grids are commonly used to discretize the computational domain and the irregular boundaries are usually represented by triangular mesh in two dimensions or tetrahedron meshes in three dimensions, in which the calculated radiative heat flux can be very smooth.[14,15] Recently, there were growing interest and applications in using structured meshes for solving the problems with complex domains and boundaries. Various numerical strategies are suggested to treat the boundary conditions along the irregular wall, such as blocked-off method,[16] embedded boundary method,[17] cut-cell method,[18] immersed boundary method,[19–22] lattice Boltzmann method,[23–25] *etc*. These methods have been successfully applied to the fluid flow, heat transfer and gas–solid flow problems. Only the blocked-off method and embedded boundary method are currently available in the radiative heat transfer community for Cartesian structured grids.[16] When the blocked-off method is combined with the discrete ordinates method (DOM) or the finite volume method (FVM) to solve the radiative transfer equation (RTE), the complex walls are actually approximated as stair-like boundaries, which brings difficulties in determining the radiative heat flux at the irregular boundaries. Many researches have shown that the obtained radiative heat flux from the blocked-off method is highly oscillating[17,26] as shown in Fig. 1(a). This is partially due to the fact that the radiative heat flux is calculated on the "untrue" approximated boundaries as shown by the green lines in Fig. 1(b). There are some modifications to this issue, but the outcome is not very satisfactory.[26–31] Young Byun *et al*.[17] showed that the multiblock, blocked-off and embedded boundary method can be used to calculate the radiative heat flux on regular walls accurately, while on the irregular wall, the blocked-off method has poor accuracy. Zabihi *et al*.[26] compared the blocked-off method with embedded boundary method for radiative heat flux along the inclined boundary and curved boundary. The results show that both methods produce fluctuations, and the blocked-off method is much worser than the embedded boundary method, leading the heat flux at the circular boundary to fail to be obtained. Sun and Zhang[31] developed a coupled lattice Boltzmann method and FVM for combined conduction and radiation heat transfer problem in a complex geometry and proposed an method to calculate the radiative heat flux based on the blocked-off method. The oscillation is significantly reduced for inclined wall but still exists for curved wall. Li *et al*.[32] combined the Monte Carlo method with the blocked-off and embedded boundary method for obtaining the conduction

*Project supported by the Startup Foundation for Introducing Talent of Nanjing University of Information Science and Technology, the Anhui Provincial Natural Science Foundation, China (Grant No. 2008085ME151), and the National Natural Science Foundation of China (Grant Nos. 51976057 and 51827808).

†Corresponding author. E-mail: shuzheng@ncepu.edu.cn

© 2020 Chinese Physical Society and IOP Publishing Ltd

and radiation in irregular geometries. The blocked-off boundary treatment also yields obvious errors in radiative heat flux for curved boundaries, although it is coupled with highly accurate Monte Carlo method. This proves that its error is largely caused from the step approximation of the curved boundary.

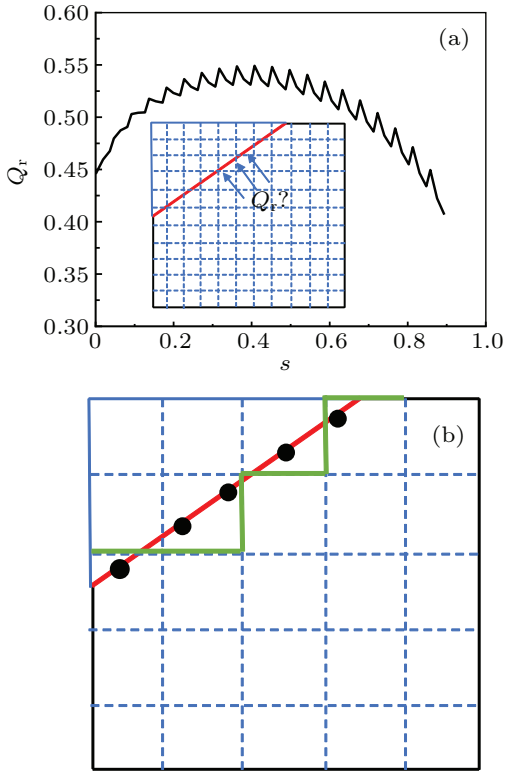


Fig. 1. Oscillating radiative heat flux at complex boundary.

In the immersed boundary method (IBM), no approximation is made for the irregular wall. Instead, several points (black circles in Fig. 1(b)) at the physical boundary are selected to represent the wall, and its interactions with other grid nodes are tackled by additional numerical treatments, which is made particularly suitable for moving boundary problems. A superior feature of the IBM is that those points can be arbitrarily placed along the boundary. Therefore, the radiative heat flux could be free of oscillation if they are calculated on these points rather than the adjacent horizontal or vertical element surfaces. To achieve this, we propose here to use the Monte Carlo method and discrete ordinates method (DOM) to directly calculate the radiative heat flux at boundary points. Monte Carlo method is now widely used in many areas.[33–38] Conventional forward Monte Carlo (FMC) and DOM have difficulties in calculating the radiative heat flux at these points. In the FMC method, energy bundles are emitted from the entire computational domain, and because the statistical nature of the Monte Carlo method, substantial energy bundles are needed to ensure that enough bundles can reach the specific points at the irregular boundary to eliminate statistical errors.[39,40] The reverse (backward) Monte Carlo (RMC) method is an effective way to reduce the computational demand with the accuracy maintained, and has been widely used to obtain high-resolution radiative intensity.[41–43] Whether for structured grids or unstructured grids, to the author's best knowledge, there is currently no method to calculate the radiative heat flux at an arbitrary point along the wall boundary.

From the above literature reviews, few methods exist to achieve an accurate radiative heat flux on irregular boundaries for tyhe structured grids. The purpose of this study is to use the RMC and DOM to directly calculate the radiative heat flux a irregular boundaries. The rest of this paper firstly presents the formulations of the RMC and DOM and their calculation procedures. Then they are applied to two benchmark problems todemonstrate their performances.

2. Mathematical models

The conservation equation of radiation in an absorbing and emitting medium is

$$\nabla I(\boldsymbol{s}) = -\kappa I + \kappa I_{\mathrm{b}}, \tag{1}$$

where $\boldsymbol{s}$ is the direction of the radiation propagation, κ is the absorption coefficient, I is the radiation intensity, and I_{b} is the blackbody emissive radiation intensity. Scattering is not considered in this work. Along a light of sight, the radiative intensity is

$$I_{\mathrm{l}} = \varepsilon I_{\mathrm{w}} \exp\left(-\int_0^l \kappa \mathrm{d}l'\right) + \int_0^l \kappa I_{\mathrm{b}} \exp\left(-\int_0^l \kappa \mathrm{d}l'\right) \mathrm{d}l', \tag{2}$$

where l is the optical length along the light of sight, ε is the wall emissivity, I_{w} is the radiative intensity at the wall, and I_{b} is the black-body emission of the participating medium. The first term on the right-hand side in Eq. (2) is due to wall emission. In this paper, the gray model is considered and it is straightforward to be extended to non-gray radiation heat transfer with an appropriate non-gray gas radiation model.[44–46]

2.1. Reverse Monte Carlo method

In the forward Monte Carlo method, numerous energy bundles are generated in the surface and inside of each element and then tracked until their energy diminishes. The Radiation heat source or heat flux are then summed over all the energy bundles for each element. Based on the principle of reciprocity, the radiation intensity at a desired location along a direction can be determined by back-track from this location to the emission point. For example, to obtain the radiative heat flux at the red point in Fig. 2(a), one can generate energy bundle from this point and then track the bundle until it is absorbed by the media or the wall. If the boundary is black, the

radiative intensity for a single ray along a specific direction can be calculated from[39]

$$I(-\boldsymbol{s}) = \int_0^l \kappa I_\mathrm{b}\,\mathrm{d}l'. \tag{3}$$

After N energy bundle emissions, the radiative heat flux can be obtained as

$$q(-\boldsymbol{s}) = \frac{1}{N}\sum_{n=1}^{N} I(-\boldsymbol{s}). \tag{4}$$

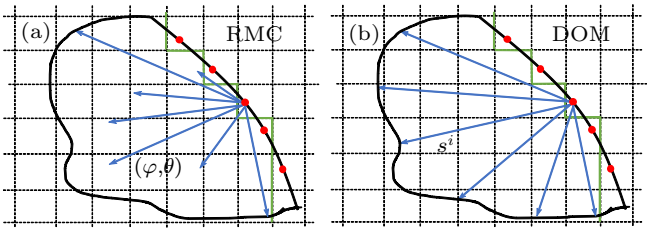


Fig. 2. Schematic diagram of heat flux calculation on irregular boundary for RMC and DOM.

The ray tracing process of RMC is similar to that of the forward Monte Carlo method and can be found elsewhere.[33]

2.2. Discrete ordinates method

The DOM or the FVM for the RTE features angular quadrature in the spherical space[47] and is described as follows:

$$\frac{\mathrm{d}I^m}{\mathrm{d}s} = -\kappa I^m + \kappa I_\mathrm{b}, \tag{5}$$

where m denotes the number of angular directions, whose total number depends on the quadrature scheme. The S6 scheme is used in this work. The application of the DOM to radiation heat transfer problems usually comes with discretization of the computational domain, solution process of the RTE for each direction on the meshes, and summation over all the direction to calculate the radiative heat source or heat flux. This is typical DOM procedures for combined problems where heat source is needed to be inserted into the energy equation.[31,34]

The idea of this work is to use the analytical solution of the DOM to calculate the heat flux along the wall boundary, thereby avoiding solving the RTE for every direction and element. In fact, the analytical solution also avoids the false scattering effect of the DOM and is also efficient in the calculating of wall heat flux. It is also worth noticing that it still has some limitations. The analytical solution is applicable to the cases without scattering, and it still suffers the ray effect due to the angular quadrature treatment, which may still induce oscillating results. This behavior will be investigated in detail. Based on Eq. (2), the incoming radiative intensity at a wall from direction m with the wall emission taken into consideration is expressed as

$$I^m = \varepsilon I_\mathrm{w} \exp\left(-\int_0^{l_m} \kappa \mathrm{d}l'\right) + \int_0^{l_m} \kappa I_\mathrm{b} \exp\left(-\int_0^{l_m} \kappa \mathrm{d}l'\right) \mathrm{d}l', \tag{6}$$

where l_m is the optical length along ray m. Then the heat flux can be obtained to be

$$q = \sum_{m=1}^{M} w^m I^m \boldsymbol{\mu}\cdot\boldsymbol{n}_\mathrm{s}, \tag{7}$$

where M is the total number of discrete ordinates, w is the angular weight, $\boldsymbol{\mu}$ is the direction cosine, and $\boldsymbol{n}_\mathrm{s}$ is the normal of the wall surface. The S6 scheme is used in this work to show the validity of the DOM, and other schemes could be used as the same procedure, the quadrate set can be found in Ref. [48]. Depending on the normal of the wall surface, about half of total 24 directions in two dimensions are needed to calculate the radiative heat flux. Typical ray directions are shown in Fig. 2(b). The difference between the RMC and DOM lies in the fact that all the rays in the DOM reach bounded wall while the energy bundle (also ray) in the RMC may end in the medium. The DOM needs significantly lower calculations than RMC and is very efficient, which will be shown in the next section.

3. Results and discussion

The validity and performance of RMC and DOM methods are demonstrated by two cases here. Two kinds of irregular boundaries are investigated, namely, inclined straight boundary and curved boundary as shown in Fig. 3. The trapezoidal and semicircular geometries are frequently used as benchmark cases for investigating radiation solvers. To focus on the calculation of radiative heat flux, all boundaries are assumed to be black and the participative part is set to be at 1000 K. Results of non-dimensional radiative heat flux along the yellow boundaries are presented and analyzed. As the absorption coefficient of the participating medium is assumed to be constant, no Cartesian grids are needed. These methods are straightforward to be extended to the cases with variable absorption coefficient and are not considered here. The optical thickness values for the two geometries are defined as and respectively, where L is the length of the bottom wall of trapezoidal enclosure and R is the radius of the outer circle of the semi-circle enclosure.

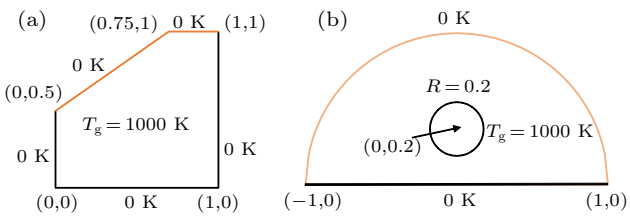


Fig. 3. Physical models of (a) inclined straight boundary and (b) curved boundary.

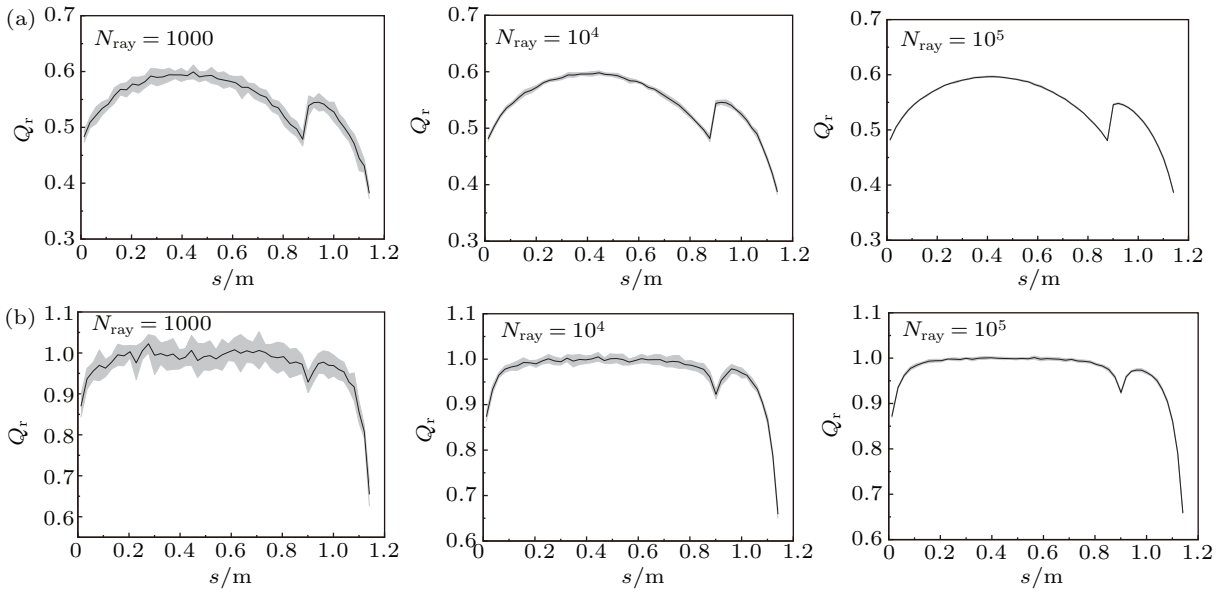


Fig. 4. Effect of energy bundles on heat flux for $\tau = 1.0$ (a) and 10.0 (b).

Figure 4 shows the radiative heat fluxes along the top boundary of the trapezoidal geometry, obtained by the reverse Monte Carlo method under different energy bunders and optical thickness values. Figure 4(a) corresponds to optical thickness of 1, while figure 4(b) for 10. The $Q_{\rm r}$ denotes the dimensionless radiative heat flux. Under both optical thickness conditions, the radiative heat fluxes will drop to their correponding local minima at the junction of the inclined and horizontal boundaries. The radiative heat flux along the inclined wall for optical thickness of 10.0 is flatter than that of 1.0 due to diffusion behavior of radiation heat transfer for optically thick condition.

Different energy bundles are adopted in the reverse Monte Carlo method to show the statistical errors of their results. The gray shaded areas along the solid lines in Fig. 4 refer to the standard deviations of the radiative heat flux for 10 samples. It can be seen that the standard deviation decreases as the number of the energy bundle increases. For 1000 energy bundles, the mean radiative heat flux is quite oscillating, but becomes smooth enough when the energy bundles increase up to 10^5. Another feature is that the standard deviation is larger for larger optical thickness condition as can be seen from the curves in the right three panels.

Figure 5 shows the comparisons among the radiative heat fluxes for DOM and RMC for three optical thickness values. The S6 quadrature set is used for the angular discretization. Results predicted by the DOM is generally larger than those by the RMC for all three cases, and show more abrupt variations at both inclined and horizontal part of the top boundary. The discrepancies between the results from the DOM and the RMC mainly originate from ray effect and their accuracies can be improved by using more energy bundles. Even so, the analytical S6 method is oscillationfree and can be seen as being accurate enough, especially in terms of the mean radiative heat flux as shown in Table 1. The error of the S6 is only about 1% relative to RMC, where the error is defined as

$$\text{Error} = \frac{\left|Q_{\rm r}^{\rm RMC} - Q_{\rm r}^{\rm DOM}\right|}{Q_{\rm r}^{\rm RMC}} \times 100\%, \tag{8}$$

where $Q_{\rm r}^{\rm RMC}$ is the mean radiative heat flux obtained by the RMC method and $Q_{\rm r}^{\rm DOM}$ by the DOM method. The calculation time of the DOM method for this case is about 3.25 ms, while the time of RMC method reaches 21 s for one sample.

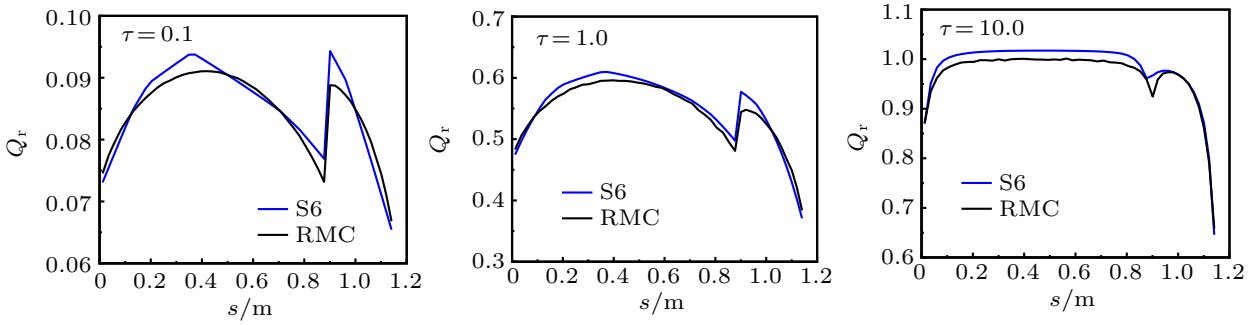


Fig. 5. Comparison between $Q_{\rm r}$ values from DOM method and RMC method.

Table 1. Mean radiative heat flux along top boundary.

τ	RMC	DOM	Error of DOM/%
0.1	0.08446	0.08497	0.6
1.0	0.54448	0.55072	1.1
10.0	0.96764	0.98196	1.8

Previous cases are limited to walls with 0 K and S6 scheme, to determine whether these two factors have significant effects on determining the radiative heat flux, additional simulations are performed for the cases of 500-K S4 scheme and S8 scheme. Figure 6(a) shows the comparison between radiative heat fluxes for wall temperatures 0 K and 500 K. When the optical thickness is 0.1, the radiative heat flux for 500 K is about 75% higher than that for 0 K, although the medium temperature is 1000 K. This is due to the fact that for optically thin condition, wall emission can propagate far away and medium emission is small. When the optical thickness is 1.0, the differences between different wall temperatures are much smaller than when optical thickness is small. For both optical thickness values, the differences between the DOM and RMC are almost the same for different wall temperatures, indicating that the wall emission has almost no effect on the performances of these two solvers.

The DOM has a shortcoming of ray effect, and the quadrature schemes may have an influence on its accuracy in calculating the radiative heat flux. Figure 6(b) shows the comparison among the S4, S6, and S8 for two optical thickness values. For the two optical thickness values, it is not easy to conclude which scheme is the most accurate since all the three schemes produce the results close to that of RMC in some regions and deviate from it in other regions, so is the curved wall case, and the comparison is not shown for that case, and we will show only the results of S6 in the subsequent sections.

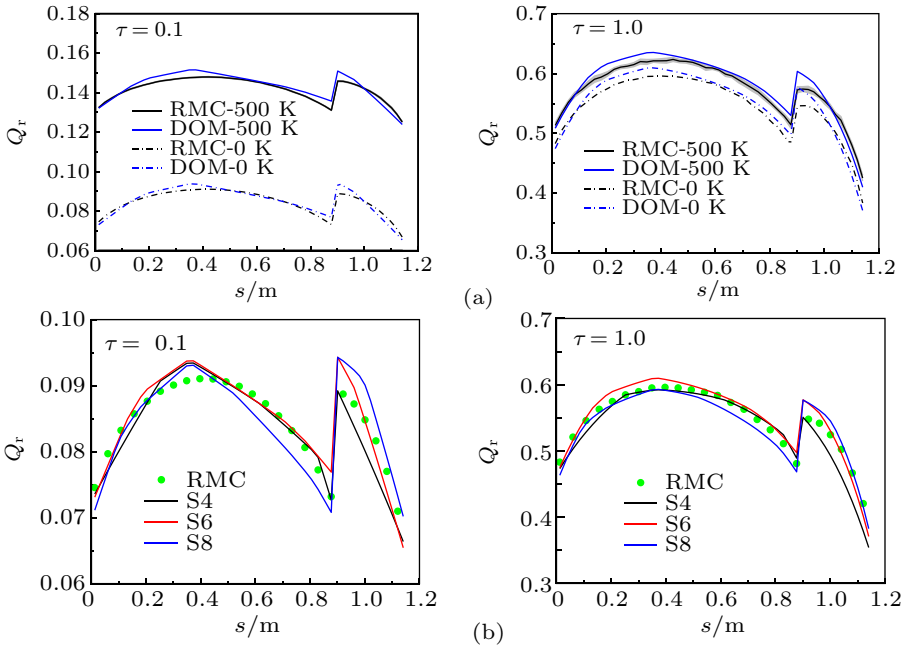


Fig. 6. Effects of (a) wall temperature and (b) DOM scheme on radiative heat flux.

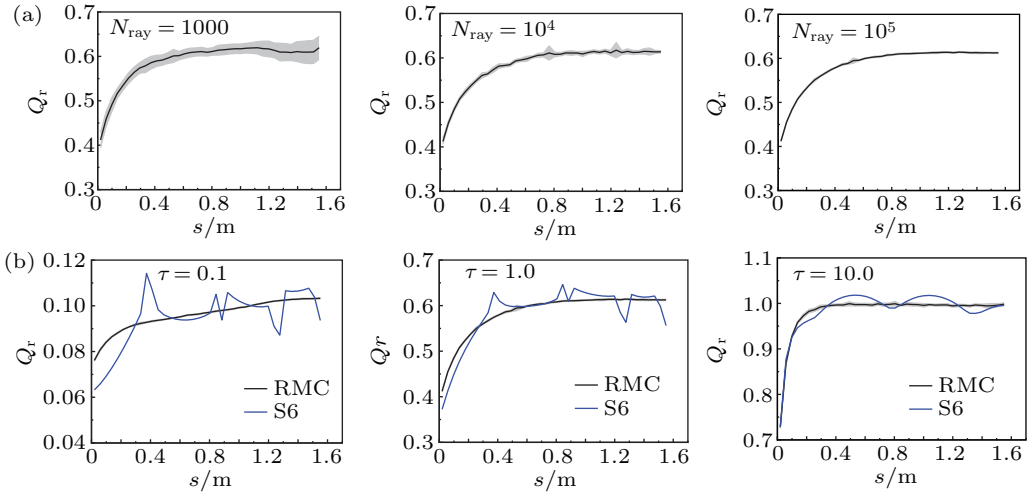


Fig. 7. (a) Comparison between radiative heat fluxes of semi-circular geometry, showing effect of energy bundles for $\tau = 1.0$, and (b) comparison between S6 and RMC.

To validate the performances of these two methods for the curved wall, figure 7 shows the radiative heat fluxes along the outer half-circular wall of the semi-circular geometry, and only half of the result is shown here due to symmetry. Figure 7(a) shows the effect of the energy bundles on the statistical error of the radiative heat flux, calculated by the reverse Monte Carlo method. Like previous trapezoidal case, when 10^5 energy bundles are emitted at the boundary, the mean radiative heat flux of 10 samples is smooth enough and the standard deviation is negligible.

As seen in these panels, the radiative heat flux increases linearly from the side to the middle and the flat region becomes larger with the increase of optical thickness. Under the optical thin condition ($\tau = 0.1$), the heat flux profile of RMC shows slight fluctuations around $s = 0.7$ m and $s = 1.2$ m, which is due to the presence of the small circle wall inside the semi-circular enclosure. Unlike the RMC, the S6 method shows significant oscillations with multiple abrupt local maxima and minima. This is caused by the inherent ray effects of the DOM due to limited angular quadrature approximations of the entire spherical space, and this effect can be reduced by increasing quadrature numbers. Compared with the case shown in Fig. 1, this phenomenon is solely related to the ray effect and much more frequent oscillations will emerge if blocked-off method is used to approximate the curved wall. Another feature is that this oscillation behavior decreases as the optical thickness increases, which is reasonable because the radiation heat transfer shows diffusion pattern for optically thick conditions, and is mainly influenced by local regions. Moreover, this fluctuation is not only limited to the curved wall, but also existent at the straight wall as shown in Fig. 8. Though this fluctuation is inevitable, the mean radiative heat fluxes of the RMC and S6 DOM are close to each other, which can be seen from Table 2. This means that the S6 can be considered as being accurate enough in terms of the mean radiative heat flux.

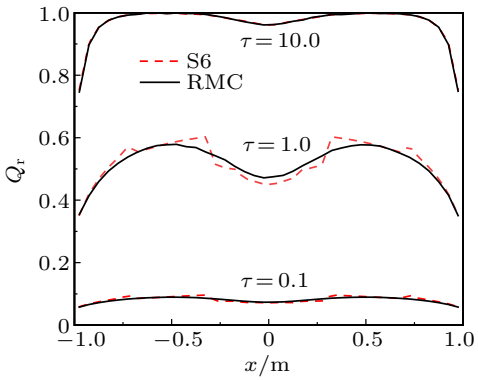


Fig. 8. Radiative heat fluxes along bottom wall for semi-circular geometry with $\tau = 0.1$, 1.0, and 10.0.

In terms of computational efficiency, the DOM is much more efficient than the RMC. For both geometries, the RMC needs tens of seconds to several minutes to converge while the DOM needs only several seconds. Although it has a limitation, the RMC is generally more preferable than the DOM due to its simple extension to the conditions with scattering media and reflecting walls.

Table 2. Mean radiative heat fluxes along top curved wall.

τ	RMC	DOM	Error of DOM/%
0.1	0.09602	0.09489	1.2
1.0	0.58449	0.58419	0.05
10.0	0.98269	0.98540	0.27

4. Conclusions

Accurate radiative heat flux prediction is important for the thermal design of high temperature devices. The reverse Monte Carlo method and analytical discrete ordinates method are proposed to calculate radiative heat fluxes at irregular boundaries, including inclined and curved boundaries. The RMC and DOM are tested for these two kinds of boundaries. The RMC can produce very smooth radiative heat flux when enough energy bundles are emitted from the boundary, while the analytical DOM shows some fluctuations, which is due to its ray effect. However, the analytical DOM is much faster than the RMC in calculation speed. For the problems where the detailed radiative heat flux profiles are needed, the RCM is better than the analytical DOM. As for the mean radiative heat flux, the analytical DOM is very accurate than the RMC, its relative error is only about 1%–2% for both inclined and curved walls. This suggest that the analytical DOM is preferred for problems where only mean radiative heat flux is important. The developed method can be further integrated with IBM for solving the combined radiation and other heat transfer problems with complex boundaries.

Although the S6 DOM can predict the accurate mean radiative heat flux compared with RMC, especially under the conditions where only total or average heat flux is needed, its oscillating heat flux profile along the boundary may cause issues under some conditions, such as in combined heat transfer problems with Neumann boundary condition or conjugate heat transfer problems. This needs further attention and now is under study.

References

[1] Yang X, Clements A, Szuhánszki J, Huang X, Farias Moguel O, Li J, Gibbins J, Liu Z, Zheng C, Ingham D, Ma L, Nimmo B and Pourkashanian M 2018 *Appl. Energy* **211** 523
[2] Seddighi Khavidak S, Pallarès D, Normann F, Johnsson F and Ylä-Outinen V 2015 *Int. J. Greenh. Gas Control* **37** 264
[3] Sun Y, Zheng S, Jiang B, Tang J and Liu F 2019 *Int. J. Heat Mass Transfer* **145** 118777
[4] Ates C, Ozen G, Selçuk N and Kulah G 2016 *J. Quantum Spectrosc. Radiat. Transfer* **182** 264
[5] Ates C, Sen O, Selçuk N and Kulah G 2017 *Int. J. Therm. Sci.* **122** 266
[6] Zheng S, Liang W, Chu H and Zhou H 2020 *Fuel* **266** 117061
[7] Sui R and Mantzaras J 2016 *Combust. Flame* **173** 370

[8] Sui R, Mantzaras J, Es-sebbar E and Bombach R 2019 *Proc. Combust. Inst.* **37** 5465

[9] Zheng S, Yang Y, Li X, Liu H, Yan W, Sui R and Lu Q 2020 *Fuel Process. Technol.* **204** 106423

[10] Zheng S, Yang Y, Sun R and Lu Q 2021 *Appl. Therm. Eng.* **183** 116194

[11] Liu G and Liu D 2018 *Chin. Phys. B* **27** 054401

[12] Yan J, Wang F, Huang Q, Chi Y, Cen K and Liu D 2011 *Acta Phys. Sin.* **60** 060701 (in Chinese)

[13] Du Y, Peng Z and Ding Y 2020 *Opt. Express* **28** 3482

[14] Wang C H, Feng Y Y, Yue K and Zhang X X 2019 *Int. Commun. Heat Mass Transfer* **108** 104287

[15] Zhang Y, Ma Y, Yi H and Tan H 2013 *J. Quantum Spectrosc. Radiat. Transfer* **129** 118

[16] Chai J C, Lee H O S and Patankar S V. 1994 *Numer. Heat Transfer Part B Fundam.* **26** 225

[17] Young Byun D, Wook Baek S and Young Kim M 2003 *Numer. Heat Transfer Part A Appl.* **43** 807

[18] Schneiders L, Günther C, Meinke M and Schröder W 2016 *J. Comput. Phys.* **311** 62

[19] Kim J, Kim D and Choi H 2001 *J. Comput. Phys.* **171** 132

[20] Tseng Y H and Ferziger J H 2003 *J. Comput. Phys.* **192** 593

[21] Kim J and Choi H 2004 *KSME Int. J.* **18** 1026

[22] Luo K, Zhuang Z, Fan J and Haugen N E L 2016 *Int. J. Heat Mass Transfer* **92** 708

[23] Chen Q, Zhang X and Zhang J 2013 *Phys. Rev. E* **88** 033304

[24] Zhang T, Shi B, Guo Z, Chai Z and Lu J 2012 *Phys. Rev. E* **85** 016701

[25] Sun Y and Zhang X 2016 *Int. J. Heat Mass Transfer* **97** 611

[26] Zabihi M, Lari K and Amiri H 2017 *J. Brazilian Soc. Mech. Sci. Eng.* **39** 2847

[27] Amiri H, Mansouri S H and Safavinejad A 2010 *Int. J. Therm. Sci.* **49** 492

[28] Talukdar P, Mendes M A A, Parida R K, Trimis D and Ray S 2013 *Int. J. Therm. Sci.* **72** 102

[29] Amiri H, Mansouri S H and Coelho P J 2011 *Int. J. Therm. Sci.* **50** 515

[30] Aghanajafi C and Abjadpour A 2015 *J. Brazilian Soc. Mech. Sci. Eng.*

[31] Sun Y and Zhang X 2018 *Int. J. Heat Mass Transfer* **121** 1039

[32] Li Z H, Li X L, Xia X L and Sun C 2020 *Heat Transfer Part B Fundam.* **77** 22

[33] Howell J R 1998 *J. Heat Transfer* **120** 547

[34] Sun Y, Zhang X and Howell J R 2017 *J. Quant. Spectrosc. Radiat. Transfer* **194** 31

[35] Chen R, Nie L and Chen C 2018 *Chaos* **28** 053115

[36] Chen R, Nie L, Chen C and Wang C 2017 *J. Stat. Mech.* **2017** 13201

[37] Jianqiang Z, Linru N, Chongyang C and Xinyu Z 2016 *AIP Adv.* **6** 075212

[38] Zhao H, Shi Z and Nie L 2020 *Eur. Phys. J. B* **93** 56

[39] Modest M F 2003 *J. Heat Transfer* **125** 57

[40] Xu Y P and Li S 2020 *Acta Phys. Sin.* **69** 029501 (in Chinese)

[41] Cheng Y, Li H, Zhang J and Huang Z 2020 *Int. J. Heat Mass Transfer* **152** 119475

[42] Wang D and Zhou H 2019 *J. Quant. Spectrosc. Radiat. Transfer* **226** 100

[43] Wang F, Liu D, Cen K, Yan J, Huang Q and Chi Y 2008 *J. Quantum Spectrosc. Radiat. Transfer* **109** 2171

[44] Zheng S, Sui R, Yang Y, Sun Y, Zhou H and Lu Q 2020 *Int. Commun. Heat Mass Transfer* **114** 104566

[45] Sun Y and Zhang X 2018 *Int. J. Heat Mass Transfer* **121** 819

[46] Sun Y, Ma J, Yu Y, Ye B and Gao C 2019 *J. Quantum Spectrosc. Radiat. Transfer* **236** 106600

[47] Modest M F 2013 *Radiative Heat Transfer* (New York: Academic Press)

[48] Howell J R, Menguc M P and Siegel R 2010 *Thermal Radiation Heat Transfer* (Boca Raton: CRC press)